Sodium Heat Transfer Correlations and Thermal Effect on EBR-II SHRT-17 Analysis

Andong SHIN*, Yong Won Choi
Korea Institute of Nuclear Safety, 62 Gwahak-ro, Yuseong-gu, Daejeon, Korea
**Corresponding author: andrew@kins.re.kr*

1. Introduction

EBR (Experimental Breeder Reactor)-II had implemented lots of tests for the SFR (Sodium Cooled Fast Reactor) transients. SHRT (Shutdown Heat Removal Test)-17 is one of EBR-II tests for safety demonstration of metal fueled SFR. Importance of the test is that the EBR-II tests are scheduled to be used for the V&V of MARS-LMR code, which is a safety analysis code for the DBAs of Prototype Generation-IV Sodium cooled Fast Reactor (PGSFR).

SFR version of TRACE (TRACE-SFR) [1] code is being developed and maintained by KINS since 2012 to prepare audit calculation for the future PGSFR licensing review. SHRT-17 was assessed using modified TRACE Ver.5 Patch2 for the IAEA Coordinated Research Project (CRP) on "Benchmark Analyses of EBR-II Shutdown Heat Removal Tests" [2]. Main issue of the analysis was higher system coolant flow estimation during natural circulation phases. To resolve the issue, TRACE-SFR code was assessed for hydraulic test especially for wire-wrapped fuel bundle pressure drop at first. [3] Current Version of TRACE-SFR code was upgraded based on the TRACE Ver.5 Patch 4 [4] with additional 6 sodium heat transfer correlations.

In this paper, EBR-II system response by sodium heat transfer model was analyzed for the SHRT-17 case including steady-state condition and transient temperature estimation of core channel outlet and clad surface temperature.

Current TRACE-SFR code model of EBR-II, minimum heat structures were used for conservative channel temperature result. For the auditing model, core heat structure modeling effect, such as assembly hex-duct and upper and lower shield was also considered in this study. In addition to the core heat structure model, heat transfer between subassemblies through the modeled hex-can was also studied. Hex ring inner core modeling methodology was used for the heat transfer between core channels, in which inner core subassemblies were modeled with channels by hex ring rows and assembly types.

2. Sodium heat transfer models

Original TRACE code have Lion-Martinelli correlation for sodium wall heat transfer.

- TRACE code correlation

$$\mathrm{Nu} = 4.8 + 0.025\mathrm{Pe}^{0.8}$$

For the fuel bundle and heat exchangers, more accurate heat transfer models could be used. So, shell side heat transfer (HT) correlations were surveyed and implemented into the TRACE-SFR code as optional model.

2.1. Added heat transfer correlations for TRACE-SFR code [5]

In addition to the current Lion-martinelli correlation of TRACE-SFR code, 6 sodium heat transfer models were surveyed and implemented into the code. These correlation are Mikityuk, Ushakov et al., Graber and Rieger, MARS-LMR code's Modified Schad, Borishanskii and Westinghouse (WH) correlations. Most of these correlations are function of Pe (Peclet number) and *x* (Pitch to diameter ratio).

Optional Sodium heat transfer correlations can be selected by "command line argument" option like "--na_ht*n*", where *n*=1 for Mikityuk, *n*=2 for Ushakov, *n*=3 for Graber, *n*=4 for Modified schad , *n*=5 for Borishanskii and *n*=6 for WH correlation.

3. Hex ring inner core modeling

Liquid sodium is supplied into the EBR-II system core from the core inlet plena. Inlet Plena are composed with high pressure (HP) plenum and low pressure plenum. For the outer core mainly composed of blanket and reflector sub-assemblies (SA), coolant is supplied from the lower pressure plenum. SAs in the inner core and extended core regions are received sodium from the HP plenum, accounting for about 85% of the total primary flow.

Inner core is composed of Driver (D), H (High flow driver), P (Partial Driver), S (Safety), C (Control), Steel, R (Reflector) SAs. Total number of inner core SA is 127. Except the HC (Hottest SA Channel) and instrumented SAs such as XX09, XX10, other 124 SAs are categorized as Table I by the hex ring row number for the inner core model.

Table I: EBR-II inner core SA categorization by hex ring row

Hex ring Row #	SA Types	SA Avg. Flow(kg/s)	SA #	Modeled Ch. Name
1	P	3.929	1	ring1-1
2	D	7.699	6	ring2-1
3	D	6.479	10	ring3-1
	S	5.862	2	ring3-2

4	D+P	4.963	18	ring4-1
5	C	3.022	9	ring5-1
	D+P	3.8595	7	ring5-2
	Steel	0.715	6	ring5-3
6	D,H,P	3.611	27	ring6-1
	R	0.171	2	ring6-2
7	Steel	0.323	1	ring7-1
	R	0.203	35	ring7-2
Total			124	

Basic concept of the Hex ring inner core model is that inner core SAs are categorized by location from the center of the reactor core as shown in Fig. 1. In the core ring model, ring 2-1 is surrounded by ring3-1, ring3-2 and ring1-1 channels for example. Core SA categorization methodology by arranging SAs based on the location make it possible to configure heat transfer chain between core channels.

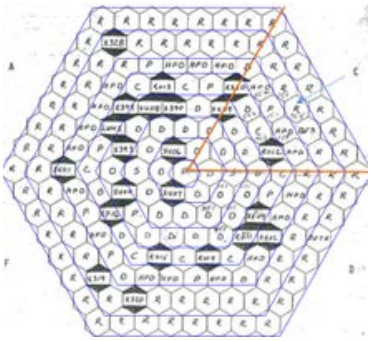

Fig. 1. Hex ring core modeling concept

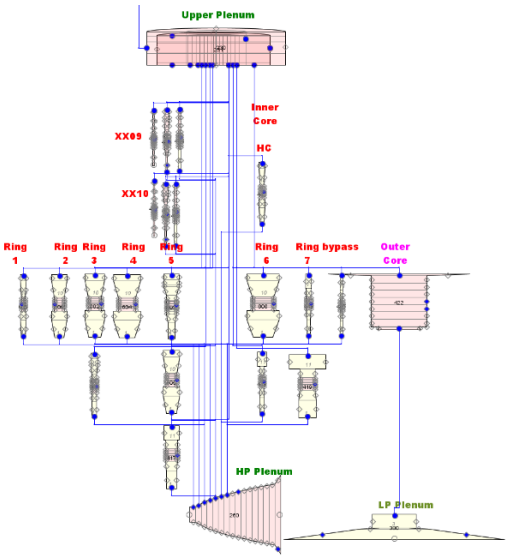

Fig. 2. TRACE-SFR code Hex ring inner core model

High pressure plenum (HP) is tube bank geometry in which sodium flows from the outside toward the center across 16-row tube columns composed of 637 interconnecting tubes. In the model, HP was modeled with the 16-cell 1D pipe component that each cell representing each row of hex tube ring as like hex core ring model.

Heated coolant through the SAs flows into the upper plenum. For detailed calculation, the upper plenum was model with 8(r) x 1(t) x 4(z) 2D component as shown in Fig. 2 TRACE-SFR code modeling for Hex ring inner core model.

4. SHRT-17 assessment result

4.1. Heat transfer correlation effect on Steady-State

Using seven different sodium HT correlations for the steady-state calculation, system power and flow is maintained stable. One of major differences is the temperature difference between bulk coolant and clad outer surface. Other difference is occur at the IHX (Intermediate Heat eXchanger) since intermediate flow was controlled to adjust IHX shell side outlet temperature in the calculation.

Fig. 3 shows the maximum temperature difference of clad outer surface and bulk coolant of each HT correlations for the HC. The maximum temperature difference was calculated for the WH correlation and minimum was for Ushakov correlation. Temperature difference of two correlations was 8.8K

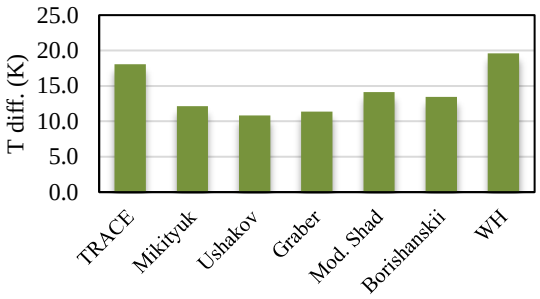

Fig. 3. Maximum Temperature difference between clad and coolant for the HC

Calculated difference of intermediate side sodium flow for each HT correlations was also similar result. The maximum intermediate side flow was for WH and minimum for Ushakov correlation. Flow difference between above two correlation was 5.3 kg/s. Lion-Martinelli correlation of TRACE code showed similar to the WH correlation case.

4.2. Heat transfer correlation effect on transients

Hex ring core model for EBR-II was used for SHRT-17 case simulation with 7 HT correlations. Based on WH HT correlation case, other HT correlation cases were compared in terms of the inner core inlet (HP) and HC flows, HC maximum coolant and clad surface temperature as Table II. Negative value means the calculated value with other HT correlation is greater than the WH HT case.

Comparison result showed that Ushakov correlation estimated lower system flow and higher SA coolant and clad temperature than WH correlation. And initial clad temperature estimation by HT correlations was diminished in the beginning phase of the transient as shown in Fig. 4 of HC clad surface temperature difference from WH correlation case. So the HT correlation effect was limited around 1% and below 1K for each flow and temperature estimations.

Table II: Core inlet and HC flow and temperature difference between WH and other heat transfer correlations

HT correlations	HP diff.	HC diff.		
	Flow	Flow	Na T	Clad T
	(%)	(%)	(K)	(K)
TRACE	0.8	0.6	-0.21	-0.06
Mikityuk	1.0	0.7	-0.65	-0.71
Ushakov	**1.1**	**0.9**	**-0.81**	**-0.84**
Graber	1.0	0.8	-0.69	-0.74
Mod. Shad	0.7	0.5	-0.39	-0.52
Borishanskii	0.9	0.7	-0.76	-0.76

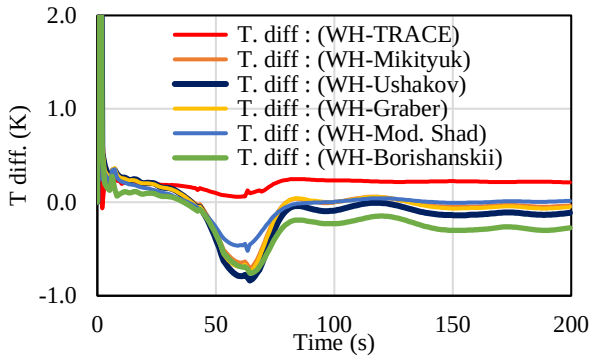

Fig. 4. HC clad temperature difference comparison of HT correlations against WH's

4.3. Effect of core heat structure modeling and heat transfer between core channels

The EBR-II model (No-HS case) is neglecting passive heat structures (HS) such as SA hex-can, upper and lower shield structures for fuel SAs considering that these passive heat structures could be a heat sink during transient.

To justify this assumption, passive HS modeling case (HS case) were assessed. In addition to the HS modeling case, one more case (HS-HT case) were assessed that heat transfer is considered between core-channels through the modeled hex can.

Heat transfer path of each ring channels are only through inner and outer core ring channel radial surfaces. Other hex-can HSs are not participating SA heat transfer and remained as passive HSs. Core channel heat transfer chain is connected from the center ring to outer core channels except HC, and instrumented drivers.

HP flow difference between above HS cases showed that HS case estimated 7.5% lower HP flow than No-HS case and HS_HT case estimated 9.3% lower flow. For the HC flow difference, the HS case also estimated 7.5% lower flow and the HS_HT case 6.2% lower than the No-HS case maximum.

HC temperature estimation results for the channel outlet temperature and the maximum coolant temperature at the top of core location are showed in Fig. 5. HC temperature estimation showed that the channel outlet temperature was decreased by the heat structure modeling cases around by 40K but HC maximum coolant temperature was increased by 16.2K and 11.9K for each HS case and HS-HT case than the No-HS case.

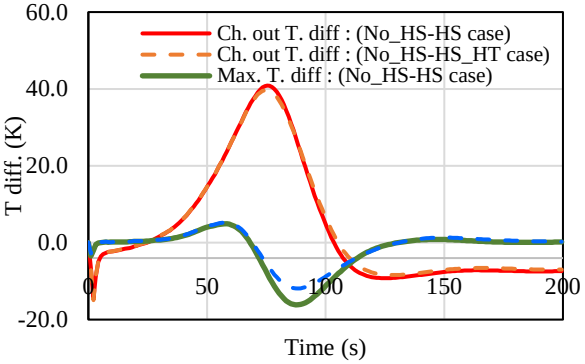

Fig. 5. HC temperature differences of the channel outlet and maximum coolant temperature by the core heat structure and the core channel heat transfer cases

Channel outlet temperature and maximum coolant temperature of each fuel ring channels during SHRT-17 transient calculations are compared in Fig. 6. Channel outlet temperatures of the core HS modeled cases were decreased around 30K than the No-HS case. But for the maximum coolant temperatures of the core HS cases, the HS-case was estimated 6K higher temperature and the HS-HT case estimated only 4K higher temperature than the No-HS case.

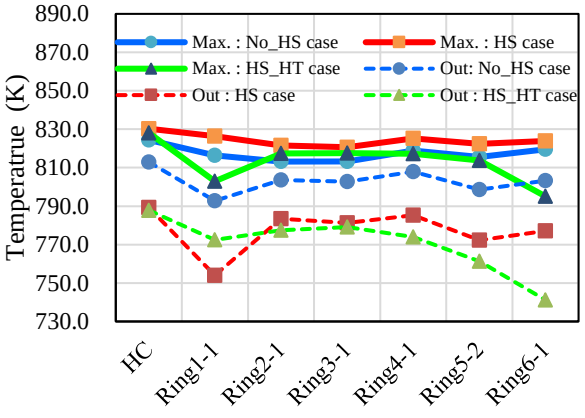

Fig. 6. Estimated SHRT-17 transient peak outlet temperature and maximum temperatures of the major core ring channels

HC was calculated with condition that the channel outer surface is adiabatic even in the HS-HT case. So the maximum coolant temperature of HC was influenced by the decreased channel flow. The Hottest coolant temperature was calculated at the HC among other inner core ring channels with the adiabatic condition of the channel.

Transient flow of HC was also influenced by the total core inlet flow (HP inlet) flow. But the influenced level of the HC flow by heat structure modeling and core channel heat transfer was not the identical to the HP flow difference level due to the flow re-distribution between core ring channels.

Axial temperature distribution of the HC at the time of coolant temperature peak for the No-HS and the HS cases are compared in Fig. 6. Coolant temperatures for the HS-case is affected by the hex-can HS modeling. Below the axial maximum temperature elevation, hex-can temperature is similar or slightly higher than coolant temperature. At the upper shield location, shield surface temperature is lower than the coolant temperature. Above the active fuel zone, HSs like hex-can and upper shield structure decreased the channel outlet temperature. Due to the core outlet temperature drop by HS modeling also affected the upper plenum temperature drop that reduce the driving force of the system natural circulation flow. This is could be the reason of the lowest core inlet flow estimated for the HS-HP case during natural circulation phase.

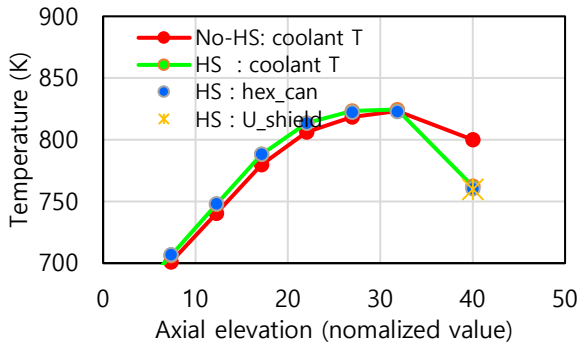

Fig. 6. Axial temperature distribution of HC at the time of coolant temperature peak for the No-HS and the HS cases

5. Conclusions

Expanded six heat transfer correlations of TRACE-SFR code were assessed for EBR-II SHRT-17 case to identify their effect on the transient. Normal clad temperature and IHX performance was affected by different heat transfer correlations. But during transient, different normal clad temperatures decreased rapidly at the beginning of transient by the core power drop and resulted that the maximum estimation difference of the core flow and HC temperatures were limited below 1% and 1K each for 6 HT correlations.

Core thermal effect was also studied for the core heat structure model and the core channel heat transfer model using the inner core hex-ring modeling methodology.

Comparing the individual core channel and total flows and channel temperature estimations with the model neglecting subassembly hex-can and fuel assembly shield structure, the core heat structure modeled case and the core channel radial heat transfer case estimated 7.5%, 9.3% lower flow each.

Analysis result showed that core channel outlet temperatures is decreased by the heat transfer of hex can and upper shield heat structure and resulted in decreased system natural circulation flow.

For the hottest coolant temperature estimation, the hottest sub-assembly channel (HC) was assumed the highest rank fuel assembly in terms of the normal power to flow ratio. Assessment result showed that the HC assumption was validated since the maximum temperature was calculated at the HC without heat transfer consideration between neighboring channels. Considering the realistic heat transfer between core channels, the hottest channel might be one of core center channels than the HC located in the core outer region even though its initial power to flow ratio is the highest.

ACKNOWLEDGEMENTS

This work was supported by the Nuclear Safety Research Program through the Korea Foundation Of Nuclear Safety (KOFONS), granted financial resource from the Nuclear Safety and Security Commission (NSSC), Republic of Korea (No. 1602003)

REFERENCES

[1] A. Shin. et al, Development of Wire-wrapped Fuel Bundle Pressure Drop Correlations for TRACE-SFR Code and Evaluation of KAERI Pressure Drop Experiments for Validation, KINS/RR-1507, KINS, 2016

[2] Benchmark Specifications and Data Requirements for EBR--II Shutdown Heat Removal Tests SHRT-17 and SHRT-45R, ANL-ARC-226(Rev1), May 31, 2012

[3] A. Shin. et al, Development of Wire-wrapped Fuel Bundle Pressure Drop Correlations for TRACE-SFR Code and Evaluation of KAERI Pressure Drop Experiments for Validation, NSAR-16NS22-17, KINS/RR-1507, NSSC, Dec 2, 2016

[4] TRACE V5.0 Theory Manual – Field Equations, Solution Methods, and Physical Models, U.S NRC, 2013

[5] A. Shin. et al, Developmental Status of TRACE-SFR code for the DBA assessment of SFR, Transactions of the KNS spring meeting, KNS, May 18, 2017